CircPTK2 Inhibits the Tumorigenesis and Metastasis of Gastric Cancer by Sponging miR-134-5p and Activating CELF2/PTEN Signaling

Huining Fan
Shanghai Jiao Tong University Affiliated Sixth people's Hospital
Xiang-Yun Zhao
Shanghai Jiao Tong University Affiliated Sixth people's Hospital
Rui Liang
Shanghai Jiao Tong University Affiliated Sixth people's Hospital
Xiao-Yu Chen
Shanghai Jiao Tong University Affiliated Sixth people's Hospital
Jing Zhang
Shanghai Jiao Tong University Affiliated Sixth people's Hospital
Ni-Wei Chen
Shanghai Jiao Tong University Affiliated Sixth people's Hospital
Jin-Shui Zhu (zhangjing5522724@alumni.sjtu.edu.cn)
Shanghai Jiao Tong University Affiliated Sixth people's Hospital https://orcid.org/0000-0002-9412-3567

Primary research

Keywords: Circular RNA PTK2, miR-134-5p, CELF2, PTEN, proliferation, metastasis, Gastric cancer

Posted Date: May 17th, 2021

DOI: https://doi.org/10.21203/rs.3.rs-514065/v1

Abstract

Background: CircRNAs are a new subset of noncoding RNAs formed by covalent closed loops and play crucial roles in the regulation of cancer gene expression. However, the roles and underlying mechanisms of circRNAs in gastric cancer (GC) remain indistinct. This study aimed to explore the role and mechanism of hsa_circ_0006421 (circPTK2) in GC.

Methods: The differential expression of circRNAs between GC tissues and adjacent normal tissues were identified by a circRNA expression profiling. Associations of circPTK2 or miR-134-5p expression with clinicopathological characteristics and prognosis of GC patients were analyzed by chi-square of Fisher's exact tests and Kaplan-Meier analysis. CCK8, colony formation, EdU assays and animal models were performed to assess the effects of circPTK2 on proliferation and invasion of GC cells. CircPTK2-specific probes were used to purify the RNA pulled down from the circPTK2, and enrichment of circPTK2 and miR-134-5p was detected by qRT-PCR. The effects of circPTK2 on miR-134-5p expression and CELF2/PTEN signaling were examined by qRT-PCR and Western blotting analysis.

Results: Low expression of circPTK2 and high expression of miR-134-5p were related to the poor survival, and high expression of miR-134-5p was related to the tumor recurrence in GC patients. Overexpressing circPTK2 suppressed the proliferation, colony formation, DNA synthesis and cell invasion as well as xenograft tumor growth and lung metastasis *in vitro* and *in vivo*, whereas silencing circPTK2 had the opposite effects. Moreover, circPTK2 was negatively correlated and co-localized with miR-134-5p in the cytoplasm of GC tissue cells. circPTK2 bound to and sponged miR-134-5p in GC cells, and miR-134-5p facilitated cell growth and invasion but attenuated circPTK2 induced tumor suppressive effects and CELF2/PTEN signaling activation in GC cells.

Conclusions: circPTK2 functions as a tumor suppressor in GC by sponging miR-134-5p and activating the CELF2/PTEN axis.

Background

Gastric cancer (GC) is a common tumor of the digestive system, which is a threat to human health worldwide [1]. According to global cancer statistics, GC is the the third leading cause of cancer-related deaths, and the incidence of which is the fifth [2]. Despite the use of digestive endoscopy in the diagnosis and treatment of GC, the prognosis of the patients is still poor, owing to tumor recurrence and metastasis [3]. The 5-year survival rate of GC is 27.4% in China [4]. Therefore, identifying promising biomarkers is essential for the early detection and mortality reduction of GC. The dysregulation of coding RNAs or noncoding RNAs is involved in the pathogenesis of GC; thus, these RNAs have potential as predictive markers for GC patients [5].

Circular RNAs (circRNAs), a new subset of noncoding RNAs, are highly conserved across species owing to their resistance to RNase R and are characterized by their covalently closed loop structures with neither a 5' to 3' polarity nor a polyadenylated tail [6]. They are considered to be RNA transcripts generated by the

back-splicing of a single pre-mRNA and possess the potential to regulate gene expression [7, 8]. The critical regulatory mechanisms of circRNAs include modulating RNA-binding proteins, sponging microRNAs (miRNAs), and participating in RNA expression and protein translation [9–11]. Owing to their stable structure, long half-life, and rich abundance in tumor tissues in comparison with linear RNAs, a large number of circRNAs are involved in many biological processes, including tumor initiation and development [12], and have become new candidate biomarkers for disease diagnosis [13]. In addition to their use in the early diagnosis of GC [14], circRNAs can also function as miRNA sponges or interact with RNA-binding proteins [12, 15].

Currently, circRNAs are known to function as tumor suppressors or oncogenes in GC progression [12, 16]. Some circRNAs have been reported to be associated with several hallmarks of diseases, including cancer cell death and survival, invasion, metastasis, and angiogenesis, as well as with disease progression and prognosis [17–20]. These circRNAs tend to be aberrantly expressed in GC, where they regulate the carcinogenesis and progression of GC [13]. For instance, hsa_circ_0000190 [21], hsa_circ_0003159 [22], and hsa_circ_000467 [23] showed increased expression in GC tissue samples, whereas hsa_circ_002059 [24] and hsa_circ_KIAA1244 [25] are down-regulated in GC tissues and plasma samples. Circ_0000993 [26], circ_000146 [27], and circ_104916 [28] inhibit GC cell proliferation and invasion by sponging miR-214-5p/-548 or regulating Slug-mediated epithelial-mesenchymal transition (EMT).

We previously proposed that circular RNA La-related protein 4 (circLARP4) acts as an anti-oncogene in GC [29], while circular RNA dihydrolipoyl succinyltransferase (circDLST) act as a tumor-promoting factor [14]. Herein, we identified a significantly down-regulated hsa_circ_0006421 in GC by circRNA profiling, which was derived from the linear gene protein tyrosine kinase 2 (*PTK2*) (chr8:141889569–141935848) and named circPTK2. However, the role of circPTK2 in GC remains unclear. In this study, we verified the effect of circPTK2 on GC cells growth and metastasis in *vitro* and in *vivo* and assessed its clinical prognostic value.

Materials And Methods

Clinical data

Clinicopathological data (age, sex, pathological stage, and so on) of 384 GC patients were downloaded from the The Cancer Genome Atlas 2015 RNA sequencing database (http://xena.ucsc.edu/getting-started/), together with relative expression levels of miRNAs (miR-495-3p, miR-134-5p, miR-221-3p, and miR-222-3p) in 41 paired tumor tissue samples and corresponding adjacent normal tissues. A human tissue microarray containing 90 paired tumor and corresponding adjacent normal tissues from GC patients (Cat HStmA180Sull) was purchased from the Shanghai Outdo Technology Co., Ltd. (Shanghai, China). Five frozen GC specimens from endoscopic biopsy were stored in liquid nitrogen in our laboratory. When we assessed the expression of miR-134-5p in GC, the inclusion criteria for patients were that as many GC cases as possible were downloaded from the TCGA cohort. When we assessed the association of miR-134-5p with the prognosis in GC, cases without the survival or recurrence information were

excluded, and the cases left (300 GC patients) were used for clinical prognostic analysis. All experiments were approved by the Ethics Committee of Shanghai Sixth People's Hospital (Shanghai, China). Histological type and clinical stage of specimens were classified according to the 2010 International Union against Cancer/American Joint Commission on Cancer (UICC/AJCC) TNM Staging Criteria (7th edition).

CircRNA microarray analysis

The differential expression of circRNAs was detected by circRNA microarray as previously reported [29]. In brief, total RNA was extracted from 5 paired GC tissues by using TRIzol (Invitrogen, Carlsbad, CA, USA) and quantified using a NanoDrop ND-1000 (Ultramicro spectrophotometer, NanoDrop, Waltham, MA, USA). Sample preparation and microarray hybridization were conducted according to the Arraystar's standard protocols (Arraystar, Waltham, MA, USA).

Identification of the targets of miR-134-5p

CircNet (http://circnet.mbc.nctu.edu.tw/) was used to screen the binding sits between circPTK2 and miRNAs. We used StarBase v2.0 (http://starbase.sysu.edu.cn) to identify the targets of miR-134-5p in cancer tissues based on the rigorous screening criteria, including identification by two prediction algorithms (Pctar and miRanda), very high stringency (> 5), and expression in at least three types of cancer.

Cell culture

Normal human gastric epithelial cell line GES-1 and GC cell lines (SGC-7901, MKN-28, HGC-27, MGC-803) were obtained from the Laboratory of Digestive Disease of Shanghai Sixth People's Hospital. All of the cells were cultured in RPMI-1640 medium (Gibco, Grand Island, NY, USA) supplemented with 10% heat-inactivated fetal bovine serum (FBS), 100 U/mL of penicillin, and 100 μg/mL of streptomycin (Invitrogen). Cells in this medium were seeded in the culture flask and cultured in an atmosphere containing 5% CO_2 and saturated humidity at 37°C.

Cell proliferation assay

Cell proliferation in GC cell lines (MKN-28, HGC-27, MGC-803, SGC-7901) was detected using a Cell Counting Kit-8 (CCK8) assay (MedChemExpress, Shanghai, China). Approximately 3×10^3 cells were seeded in each well of a 96-well plate. Each group of cells was set with 8 replicates. The edges of each well were filled with sterile phosphate-buffered saline (PBS), and cells were incubated in an atmosphere containing 5% CO_2 and saturated humidity at 37°C for 0-72 h. Then, 10 μL of CCK8 solution was added directly to each well on specified date. Then, the cells were incubated at 37°C for 0.5-4 h, and the optional density was measured at 450 nm. And the cell proliferation rate was calculated by OD (OD of test group - OD of control group / OD of control group × 100%))

Colony formation assay

After GC cells were transfected with the indicated lentivirus (MKN-28 and MGC-803), mimics (MKN-28 and MGC-803), inhibitor (HGC-27 and SGC-7901), or small interfering RNA (siRNA) (HGC-27 and SGC-7901) for 48 h, 1×10^3 cells in each group were seeded in a 6-well plate and incubated at 37°C. Medium was changed every 2 days. The cell proliferation was observed, and the culture was terminated when visible colonies appeared in the 6-well plate. Then, all cells were fixed in 2 mL 4% paraformaldehyde for 15 min and stained with a crystal violet solution for 15 min. Cell colonies were then counted and analyzed.

5-Ethynyl-20-deoxyuridine (EdU) incorporation assay

After GC cells were transfected with the abovementioned plasmids for 48 h, we used a Cell-Light EdU DNA Cell Proliferation Kit (ThermoFisher, Shanghai, China) to detect the DNA synthesis according to the manufacturer's instructions. Cells were seeded in 96-well plates (1×10^4 cells/well), with three replicates for each group. After incubation with 100 μL 50 μmol/L EdU for 2 h, 50 μL 4% paraformaldehyde was added to each well of the 96-well plates to fix the cells, and the cells were then stained with Apollo Dye Solution. PBS (100 μL) containing 0.5% TRitouX-100 was added to each well of the 96-well plates to increase the membrane permeability. Hoechst-33342 reaction solution was added to the 96-well plates to stain the nucleic acids. Olympus IX73 microscope (Olympus, Tokyo, Japan) was used to collect the images, and the proportions of EdU-positive cells were calculated.

Transwell invasion assay

After GC cells were transfected with the abovementioned plasmids for 48 h, the cell invasion assay was performed using 24-well Transwell insert chamber plates (Corning Costar, 8.0 μm pore size). The Matrigel (BD, San Jose, CA, USA) and serum-free medium were mixed on ice at a ratio of 1:4 to prepare appropriated Matrigel solution, 50 μL of which was evenly spread on the upper surfaces of transwell chamber. Cells (1×10^4/group) in 200 μL of serum-free RPMI-1640 medium were added to the upper chamber. A total of 500 μL of RPMI-1640 medium supplemented with 10% FBS was added into the lower chamber incubated at 37°C. After 48 h, the invaded cells in the upper chamber were gently wiped with a cotton swab, fixed with 4% paraformaldehyde for 15 min, stained with a crystal violet solution at room temperature for 30 min, and gently rinsed with PBS twice. The cells were then observed, photographed, counted, and analyzed.

Transfection of siRNA, overexpression lentiviruses, mimics and inhibitor

siRNAs targeting the junction region of circPTK2 (sense: 5'-AGAGGAGUGGAAGCAGAACTT-3'; antisense: 5'-GUUCUGCUUCCACUCCUCUTT-3') and circPTK2-overexpressing lentivirus were synthesized by GenePharma (Shanghai, China). MGC-803 and SGC-7901 cells were transfected with si-circPTK2, and MKN-28 and HGC-27 cells were transfected with the circPTK2-overexpressing lentivirus using transfect-mate (GenePharma) according to the manufacturer's instructions. miR-134-5p mimics or control mimics and inhibitor or control inhibitor were synthesized by GenePharma (Shanghai, China).

Actinomycin D and RNase R treatment

Actinomycin D and RNase R were used to detect the stability of circPTK2. In brief, 2 mg/mL actinomycin D or dimethyl suffoxide (DMSO) (Sigma-Aldrich, Sr. Louis, MO, USA) was added to the transcription of HGC-27 and MKN-28 cells, and DMSO was the negative control. After incubation for 24 h, the expression levels of *PTK2* and circPTK2 were detected by quantitative real-time PCR (qRT-PCR). RNase R (3 U/μL, Epicentre Technologies, Madison, WI, USA) was added to the RNA (2 μg) of MGC-803 and MKN-28 cells respectively, and then incubated for 30 min at 37°C. Then, the RNA expression levels of *PTK2* and circPTK2 were detected by qRT-PCR.

Luciferase reporter assay

Luciferase reporter assay was used to verify the binding site between circPTK2 and miR-134-5p. The luciferase reporter vectors were constructed by GenePharma. The luciferase reporter vector and internal reference were co-transfected in HEK293T cells (Chinese Academy of Sciences, Shanghai, China) in 96-well plates by using the transfect-mate transfection reagent. After 48 h, the fluorescence value was determined with a dual-luciferase reporter assay (Promega, Georgia, Madison, USA). Cell lysis (10 μL) was added to 40 μL of LAR II, then mixed, and measured the reading, which was the value of Firefly Luciferase. Then, 40 uL Stop&Glo was added and read again, which was the value of Renilla Luciferase. The ratio of two sets of data was calculated.

qRT-PCR

The RNA expression levels of circPTK2 and miR-134-5p were detected by qRT-PCR. Total RNA was extracted from the GC cells using TRIzol reagent (Invitrogen, Waltham, MA, USA). Evo M-MLV (Thermo Fisher Scientific, Waltham, MA, USA) was used to reversely transcribe RNA, and SYBR Green Master Mix kit (Takara, Otsu, Japan) was used for cDNA amplification. The amplification reaction conditions were as follows: 95°C for 30 s, 60°C for 30 s, and 72°C for 60 s. In addition, High Pure miRNA isolation kit (Roche, Basel, Switzerland) was used to isolate total miRNA, and RT-PCR was performed using a TaqMan MicroRNA Reverse Transciption kit (Life Technologies, Shanghai, China). Primers are listed in **Supplementary Table S1**.

Western blotting analysis

Western blotting analysis was performed to determine the protein abundance in HGC-27 and MGC-803 cells. Total protein was extracted with lysates. After centrifugation (12000 rpm, 5 min, 4℃), the supernatant fluid was collected, and the concentration was measured using a Pierce BCA kit (Thermo Fisher Scientific), followed by 10% sodium dodecyl sulfate-polyacrylamide gel electrophoresis (SDS-PAGE). Polyvinylidene difluoride (PVDF) membranes (Millipore, Boston, MA, USA) were then rinsed using a blocking solution with 5% fat-free milk for 1 h at room temperature and incubated overnight at 4°C in primary antibodies, followed by incubation in secondary antibodies for 1 h at room temperature. The anti-CUGBP Elav-like family member 2 (*CELF2*) (1:1000, ab186430), anti-phosphate and tension homology deleted on chromsome ten (*PTEN*) (1:1000, ab32199), anti-proliferating cell nuclear antigen (*PCNA*)

(1:1000, ab92552), and anti-matrix metalloproteinase 2 (*MMP2*) (1:1000, ab97779, Abcam, Cambrige, England) were used as primary antibodies.

CircRNA in vivo precipitation (circRIP)

This experiment was conducted as previously reported [15]. CircPTK2-overexpressing HGC-27 cells were inoculated in a 10-cm dish. After 48 h, the specific biotin-tagged probe or control probe with a final concentration of 200 nm/L was transfected to HGC-27 cells. After 24 h, the cells were first fixed with 1% formaldehyde for 10 min, extracted with 1 mL lysate, and samples were treated with ultrasound. After centrifugation (10,000 × *g*, 10 min), the supernatant was transferred to a 2 mL centrifuge tube, 50 μL of it was preserved as the input control, and the remaining supernatant was used to incubate with a mixture of circPTK2-specific probe-streptavidin Dynabeads (M-280, Invitrogen) at room temperature overnight, with 200 μL of lysis buffer and proteinase K was used to reverse the formaldehyde crosslinking. Finally, the miRNAeasy Mini Kit (Qiagen, Dusseldorf, German) was used to extract total RNA according to the manufacturer's instructions. The RNA expression levels of circPTK2 and miR-134-5p were detected by qRT-PCR.

RNA fluorescence in situ hybridization (FISH)

The expression levels and cellular localization of circPTK2 and miR-134-5p in GC tissue samples were detected by FISH analysis. A digoxin-labeled probe sequence for circPTK2 (5'-AGCCCCAGTTCTTCCACTCCTCTGG-3') and biotin-labeled probe sequence for miR-134-5p (5'-CCCCTCTGGTCAACCAGTCACA-3') were synthesized. The FISH analysis was performed as previously reported [29].

In vivo tumor growth assay

Six-week-old NOD/SCID mice were purchased from the Shanghai Laboratory Animal Center (SLAC, Shanghai, China). MKN-28 cells (1×10^7) transfected with a circPTK2 overexpression vector or control lentivirus vector were resuspended in 200 μL of sterile PBS and injected subcutaneously into the right flanks of mice (7 mice in each group). After 30 days, the mice were euthanized, and the xenografted tumors were removed, weighed, and processed for hematoxylin-eosin (HE) staining and immunohistochemical (IHC) analysis to detect the expression of Ki-67 and CELF2. Staining intensity was accessed by using the Image-pro Plus 6.0 (Media Cybernetics) and was represented by the mean density, using the formula mena density = integrated optical density/area of interst. The animal experiments were approved by the Ethics Committee of Shanghai Sixth People's Hospital.

Caudal vein pulmonary metastasis models

Caudal vein pulmonary metastasis models were established to detect the effect of circPTK2 on the metastasis capacity of GC cells. In brief, 1×10^7 MKN-28 cells transfected with the circPTK2 overexpression vector or control lentivirus vector were resuspended in 0.1 mL PBS and injected into the

caudal vein of mice (7 mice in each group). After 30 days, the mice were euthanized, and the lung tissues were collected for HE to observe the metastasis of GC cells.

Statistical analysis

Statistical analysis was performed with GraphPad Prism 7 (La Jolla, CA, USA). Values are expressed as the mean ± standard deviation (SD). Student's *t* test and analysis of variance were used for comparisons between groups. Kaplan-Meier analysis was used to assess the association of circPTK2 or miR-134-5p with the prognosis in GC. Overall survival (OS) time was calculated from the date of diagnosis. Recurrence-free survival (RFS) time is defined from the treatment to tumor recurrence. A Cox proportional hazard model was used to assess the risk of circPTK2 or miR-134-5p with respect to prognosis in GC. Only the variables with statistically significant ($\alpha < 0.05$) were included in the multivariate Cox model. Pearson correlation analysis was used for the correlation between circPTK2 and miR-134-5p in GC. Categorical data were analyzed by chi-square and Fisher's exact tests. $P < 0.05$ was considered statistically significant.

Results

Identification and characteristics of circPTK2

We had previously identified 24 differentially expressed circRNAs between GC and adjacent normal tissues by circRNA expression profiling [26]; these included hsa_circ_0006421, which was significantly down-regulated in GC tissues ($P = 0.008$, fold change = 2.726; **Fig. 1A**). According to its annotation in the Circular RNA Interactome (https://circinteractome.nia. nih.gov/index.html), hsa_circ_0006421 is derived from the linear gene *PTK2* and termed as circPTK2 (**Fig. 1B**). RNase R exonuclease significantly decreased the expression of linear *PTK2* in HGC-27 and MKN-28 cells (both $P < 0.05$), but did not affect that of circPTK2 (**Fig. 1C**). We then inspected the stability of circPTK2 after treatment with actinomycin D and found that the transcript half-life of circPTK2 exceeded 24 h, whereas that of linear PTK2 was about 6 h (**Fig. 1D**), indicating that circPTK2 was highly stable in GC cells. Furthermore, the FISH analysis indicated that circPTK2 was mainly localized in the cytoplasm of in both GC tissues and MKN-28 cells (**Fig. 1E**).

Associations of circPTK2 expression with clinicopathological characteristics and prognosis of GC patients

We firstly tested the expression of circPTK2 in five GC tissue samples by qRT-PCR. Compared with paired adjacent normal tissues, circPTK2 expression was lower in GC tissues (**Fig. 2A**). Moreover, the circPTK2 expression was decreased in GC cells compared with normal gastric cells (GES-1, **Fig. 2B**). FISH analysis was performed to validate the expression levels of circPTK2 in 90 GC tissues (**Fig. 2C**). The results showed that circPTK2 was decreased in GC tissues ($P = 0.006$) (**Fig. 2D**). Furthermore, to illustrate the relationship between circPTK2 and GC, we used Cutoff Finder (http://molpath.charite.de/cutoff/load.jsp) to determine a cutoff value (89.0) for circPTK2 expression in GC tissues and used this value to divide the

GC patients into high and low circPTK2 expression groups. As shown in **Table S2, c**ircPTK2 showed no association with the clinicopathological characteristics of patients with GC. Patients with low circPTK2 expression had shorter OS than those with high circPTK2 expression (**Fig. 2E**). Lymph node metastasis was an independent prognostic factor of OS in patients with GC, but circPTK2 was not (**Table S3**).

Association between miR-134-5p and prognosis of GC patients

We used CircNet to predict the potential target miRNAs of circPTK2 and found that four miRNAs had the potential to bind to circPTK2. Then, we analyzed the expression levels of these four miRNAs in GC and found that miR-134-5p, miR-221-3p, miR-222-3p, but not miR-495-3p, showed increased expression in both 384 unpaired tissues and 41 paired tissues (**Fig. 3A**). Increased expression of miR-221-3p or miR-222-3p showed an opposite trend with the favorable survival in patients with GC (**Supplementary Fig. S1**). Thus, miR-134-5p was used for further investigations. FISH analysis validated that miR-134-5p expression levels were significantly increased in GC tissues (**Fig. 3B, C**).

Furthermore, a cutoff value (8.63) for miR-134-5p was acquired and used to divide GC patients into high and low miR-134-5p expression groups (**Fig. 3D**). As shown in **Table S4**, miR-134-5p expression was related to tumor size in patients with GC. Kaplan-Meier analysis revealed that the GC patients with high miR-134-5p expression had shorter overall survival (OS) and recurrence-free survival (RFS) compared with those with low miR-134-5p expression (**Fig. 3E, F**). Besides, high miR-134-5p expression was significantly associated with tumor recurrence among patients with stage III-IV disease, but this relationship was not observed among those with stage I-II disease (**Fig. 3 E, F**). Elevated expression of miR-134-5p was an independent prognostic factor of poor OS (**Table S5**) and RFS (**Table S6**) in patients with GC.

Effects of circPTK2 and miR-134-5p on the proliferation and invasion of GC cells

To investigate the biological functions of circPTK2 in GC cells, we analyzed circPTK2 expression in human GC cell lines by qPCR and found that circPTK2 had a lower expression in HGC-27 and MKN-28 cells but higher expression in SGC-7901 and MGC-803 cells (**Fig. 2B**). Thus, HGC-27 and MKN-28 cells were used for the overexpression of circPTK2, and SGC-7901 and MGC-803 cells were used for the knockdown of circPTK2. We constructed circPTK2-overexpression lentiviruses with circular frames and circPTK2 sequences, and found that circPTK2 was significantly overexpressed in HGC-27 and MKN28 cells (**Supplementary Fig. S2A, B**). miR-134-5p was significantly overexpressed when miR-134-5p mimics were transfected into the HGC-27 and MKN-28 cells (**Supplementary Fig. S2C**).

Then, the effects of circPTK2 overexpression on cell proliferation, DNA synthesis, colony formation, and cell invasion were determined by CCK8, EdU, colony formation, and transwell assays. We found that circPTK2 overexpression dramatically suppressed cell viability (**Fig. 4A**), DNA synthesis (**Fig. 4B**), colony formation (**Fig. 4C**), and cell invasion (**Fig. 4D**) in HGC-27 and MKN-28 cells. However, these suppressive effects of circPTK2 were counteracted by miR-134-5p mimics (**Fig. 4A-D**).

CircPTK2 knockdown promotes the proliferation and invasion of GC cells and miR-134-5p inhibitor reverses its tumor-promoting effects

The circPTK2 siRNA transfection efficiency in MGC-803 and SGC-7901 cells was confirmed by qRT-PCR (Supplementary Fig. S4). We found that circPTK2 knockdown substantially enhanced cell viability (**Fig. 5A**), DNA synthesis (**Fig. 5B**), colony formation (**Fig. 5C**), and cell invasion (**Fig. 5D**) in MGC-803 and SGC-7901 cells. However, these tumor-promoting effects induced by circPTK2 knockdown were counteracted by an miR-134-5p inhibitor (**Fig. 5**).

CircPTK2 sponges miR-134-5p to activate the CELF2/PTEN signaling in GC cells

The qRT-PCR results showed that the miR-134-5p expression was markedly down-regulated in circPTK2-overexpresing HGC-27 and MKN-28 cells and up-regulated in si-circPTK2-transfected MGC-803 and SGC-7901 cells (**Fig. 6A**). To further verify the specific binding between miR-134-5p and circPTK2, we used a circPTK2 probe to perform an RNA in vivo precipitation assay. The circPTK2-specific probes were used to purify the RNA pulled down from circPTK2, and qRT-PCR showed that the enrichment levels of circPTK2 and miR-134-5p were significantly increased compared with controls in HGC-27 cells (**Fig. 6B**). FISH analysis indicated that circPTK2 and miR-134-5p were co-localized in the cytoplasm of GC cells (**Fig. 6C**). The expression of circPTK2 was negatively correlated with miR-134-5p expression in 90 GC tissue samples (**Fig. 6D**). The binding sites of miR-134-5p with circPTK2 are indicated in **Fig. 6E**. We further found that miR-134-5p mimics reduced the luciferase activity of the wild-type (WT) circPTK2 3'-untranslated region (UTR), but had no effect on that of the mutant (Mut) circPTK2 3'-UTR compared with the miR-NC-transfected HEK293T cells (**Fig. 6F**).

Next, we used starBase v2.0 to predict the targets of miR-134-5p and identified the seven most closely related target genes [mbt domain containing 1 (*MBTD1*), SERTA domain containing 2 (*SERTAD2*), zinc finger, DHHC-type containing 9 (*ZDHHC9*), voltage-dependent anion-selective channel protein 2 (*VDAC2*), CUGBP Elav-like family member 2 (*CELF2*), methionine adenosyltransferase 2α (*MAT2A*), and isocitrate dehydrogenases 3α (*IDH3A*)]. Among these genes, *ZDHHC9*, *VDAC2*, and *CELF2* displayed the most significantly differential expression between GC and normal tissues, of which only *CELF2* showed decreased expression in paired GC tissues (**Supplementary Fig. S4**). The binding sites of miR-134-5p with *CELF2* are indicated in Fig. 6E. We then observed that miR-134-5p mimics could reduce the luciferase activity of WT CELF2 3'UTR as compared with the control miR group but had no effects on that of the Mut CELF2 3'-UTR in HEK293T cells (**Fig. 6F**). To determine whether circPTK2 sponged miR-134-5p to regulate *CELF2* expression, we measured the expression levels of *CELF2* and its downstream phosphate and tension homology deleted on chromsome ten (*PTEN*), proliferating cell nuclear antigen (*PCNA*), and matrix metalloproteinase 2 (*MMP2*) by Western blotting. CircPTK2 overexpression considerably increased CELF2 and PTEN expression but decreased PCNA and MMP2 expression in GC cells; this effect was reversed by miR-134-5p mimics (Fig. 6G). Silencing circPTK2 decreased the expression of CELF2 and PTEN but increased PCNA and MMP2 expression; this effect could be rescued by the miR-134-5p inhibitor (Fig. 6G).

CircPTK2 inhibits *in vivo* tumor growth

After four weeks, tumor volumes were smaller for circPTK2-overexpressing MKN-28 cells than for NC-transfected cells (**Fig. 7A, B**). Tumor weight for circPTK2-overexpressing MKN-28 cells were significantly lower than those for control-transfected cells (**Fig. 7C**). Tumor formation ability (**Fig. 7D**) and Ki-67 index were decreased by circPTK2 overexpression, whereas CELF2 and PTEN index values were increased (**Fig. 7E**). In addition, caudal vein pulmonary metastasis models demonstrated that the number of lung metastatic tumors in the circPTK2 group was markedly lower than that in the NC group (**Fig. 7F**). H&E analysis showed that metastatic tumor formation ability was weaker in the circPTK2 group than in the NC group (**Fig. 7G**). These results demonstrate that circPTK2 sponges miR-134-5p to activate CELF2/PTEN signaling (**Fig. 8**).

Discussion

In this study, we identified a new down-regulated circRNA hsa_circ_0006421 derived from the linear gene PTK2 (termed as circPTK2). We investigated its down-regulation in five paired GC tissues and validated these results in 90 paired GC tissues samples. The results indicated that circPTK2 might be an anti-oncogenic factor in GC. We then found that decreased circPTK2 was related to poor survival in GC patients.

CircRNAs serve as miRNA sponges in cancer [8, 9, 30]. Studies have shown that cerebellar degeneration-related protein 1 antisense (CDR1as) [8] or circular RNA-7 (ciRS-7) [9], circular RNA Streptococcus pyogenes (circ-SPY) [9], circular RNA homeodomain interacting protein kinase 3 (circ-HIPK3) [31], and circ_012559 [32] sponge miRNAs in cancer progression. Our previous study revealed that circular RNA Yes-associated protein 1 (circYAP1) and circular RNA La-related protein 4 (circLARP4) sponged miR-367-5p/-424-5p to up-regulate p27 or large tumor suppressor 1 (*LATS1*) signaling, leading to the repression of GC [15, 29]. Moreover, multiple circRNAs from the same linear RNA, PTK2, were reported, among which hsa_circ_0003221 (that is, circPTK2) accelerated cell proliferation and inhibited cell apoptosis in GC via miR-139-3p [33]. In this study, we identified circPTK2 specific binding with miR-134-5p and confirmed the direct interaction and co-localization between circPTK2 and miR-134-5p in GC cells. Further observations showed that overexpressing circPTK2 repressed the growth and metastasis of GC cells *in vitro* and *in vivo*, whereas silencing circPTK2 reversed these effects. Our results suggest that circPTK2 might act as a sponge of miR-134-5p to inhibit gastric tumorigenesis.

Previous studies showed that up-regulation of miR-134-5p was correlated with tumor recurrence in lung adenocarcinoma and favored the metastasis and chemoresistance of lung adenocarcinoma cells [34]. However, miR-134-5p was down-regulated in osteosarcoma, where it induced its apoptosis [35]. In our study, we assessed the expression of miR-134-5p in GC and found that it displayed increased expression in GC; moreover, its high expression was an independent prognostic factor for poor survival and tumor recurrence in advanced-stage GC. Likewise, we found that miR-134-5p had a negative correlation with

circPTK2 expression and reversed the tumor-suppressive effects of circPTK2 in GC cells. These results indicated that miR-134-5p mediates circPTK2 to regulate the progression of GC.

CELF2 is an RNA-binding protein that can bind to single- or double-stranded RNA and regulate thousands of transcripts [36, 37]. Recent genomic analysis showed that *CELF2* could regulate cancer-related transcripts and prevent malignant progression [38-40]. A previous study showed that *CELF2* expression was decreased in non-small cell lung cancer (NSCLC), and its down-regulation was linked to worse clinical outcomes in patients with NSCLC [41]. In our study, we identified *CELF2* as a direct target of miR-134-5p and showed that it was decreased in GC tissues and had bound directly to miR-134-5p. It was shown that *CELF2* could inhibit the proliferation of NSCLC by activating the *PTEN* activity [41], which in turn suppressed tumor growth by down-regulating *PCNA* and *MMP2* [42]. Our results demonstrated that miR-134-5p reduces the activity of the *CELF2*/*PTEN* signaling and attenuated the promotion of this signaling by circPTK2. Our studies indicated that circPTK2 sponges miR-134-5p to activate CELF2/PTEN signaling, contributing to the suppression of gastric carcinogenesis (Fig. 8).

Some limitations of the present study should be addressed. First, the study did not determine whether circPTK2 acts by directly binding with the RNA-associated proteins to inhibit GC. Second, it did not determine whether circPTK2 could produce an inhibitory effect on GC with liver metastasis. Further studies with a larger sample cohort are required to confirm the clinical prognostic value of circPTK2 in patients with GC.

Conclusion

In summary, we identified a novel tumor suppressive circPTK2 and found that it acted as a sponge of miR-134-5p to activate *CELF2/PTEN* signaling, thereby functioning as a tumor suppressor in GC.

Abbreviations

circRNA: circular RNAs; GC: gastric cancer; OS: overall survival; RFS: recurrence-free survival; CCK8: Cell counting Kit-8; EdU: 5-ethynyl-20-deoxyuridine; FBS: fetal bovine serum; PBS: phosphate-buffered saline; TCGA: The Cancer Genome Atlas; CELF2: CUGBP Elav-like family member 2; PTEN: phosphate and tension homology deleted on chromsome ten EMT: epithelial-mesenchymal transition; circLARP4: circular RNA La-related protein 4; circDLST: circular RNA dihydrolipoyl succinyltransferase; PTK2: protein tyrosine kinase 2 ; UICC/AJCC: International Union against Cancer/ American Joint Commission on Cancer; siRNA: small interference RNAs; FISH: fluorescence in situ hybridization; aRT-PCR: quantitative real-time PCR; PCNA: proliferating cell nuclear antigen; MMP2: matrix metalloproteinase 2; circRIP: circRNA in vivo precipitation; HE: hematoxylin-eosin; IHC: immunohistochemistry; MBTD1: mbt domain containing 1; SERTAD2: SERTA domain containing 2; ZDHHC9: zinc finger, DHHC-type containing 9; VDAC2: voltage-dependent anion-selective channel protein 2; CDR1as: circRNAs cerebellar degeneration-related protein 1 antisense; ciRS-7: circular RNA-7; circ-SPY: circular RNA Streptococcus pyogenes; circ-HIPK3: circular RNA

homeodomain interacting protein kinase 3; MAT2A: methionine adenosyltransferase 2α; IDH3A: isocitrate dehydrogenases 3α; NSCLC: non-small cell lung cancer; UTR: untranslated region; WT: wild-type.

Declarations

Acknowledgments

We highly appreciate the help from Shanghai GenePharma.

Author's contributions

ZJ, ZJS, and CNW have contributed to the conception and design of this research; FHN and ZXY have conducted experiments involving in vitro cells and in vivo mouse models and clinical samples; LR and CXY participated in data interpretation, stastistical analysis, and literature research; FHN, ZJ, and ZJS have participated in the writing and revision of this manuscript. All authors agreed to be accountable for all aspects of this research work. All author read and approved the final manuscript.

Funding

Our work was supported by grants from National Natural Science Foundation of China (No. 81873143 & 82074161), Double-Hundred Talent Plan of Shanghai Jiao Tong University School of Medicine (No. 20191831) and Interdisciplinary Program of Shanghai Jiao Tong University (project number YG2021QN104).

Availability of data and materials

All data were generated or analyzed during this study are included in this published article and its additional files.

Ethicls approval and consent to participate

This study was reviewed and approved by the Ethics Committee of Shanghai Sixth People's Hospital. Informed consents were obtained from all patients or his/her guardians. All experiments involving mice were performed under the rules of Shanghai Sixth People's Hospital Animal Care and Use Committee and guidelines for the Care and Use of Laboratory Animals were seriously conducted during the whole process.

Consent for publication

Consents for publication were obtained from patients or his/her guardians.

Competing interests

The authors declare that they have no competing interests.

References

1. Global Burder of Disease Cancer Collaboration. Fitzmaurice C, Abate D, Abbasi N, Abbastabar H, Abd-Allah F, et al. Global, regional, and national cancer incidence, mortality, years of life lost, years lived with disability, and disability-adjusted life years for 29 cancer groups, 1990 to 2017: a systermatic analysis for the global burden of disease study. JAMA Oncol. 2019. Sep 27. doi: 10.1001/jamaoncol.2019.2996.
2. Bray F, Ferlay J, Soerjomataram I, Siegel R, Torre LA, Jemal A. Global cancer statistics 2018: GLOBOCAN estimates of incidence and mortality worldwide for 36 cancers in 185 countries. Ca Cancer J Clin. 2018;68:394–424.
3. Sitarz R, Skierucha M, Mielko J, Offerhaus GJA, Maciejewski R, Polkowski WP. Gastric cancer: epidemiology, prevention, classification, and treatment. Cancer Manage Res. 2018;10:239–48.
4. Gao K, Wu J. National trend of gastric cancer mortality in China (2003–2015): a population-based study. Cancer Commun (Lond). 2019;39:24.
5. Fang X, Wen J, Sun M, Yuan Y, Xu Q. CircRNAs and its relationship with gastric cancer. J Cancer. 2019;10(24):6105–13.
6. Suzuki H, Tsukahara T. A view of pre-mRNA splicing from RNase R resistant RNAs. Int J Mol Sci. 2014;15(6):9331–42.
7. Jeck WR, Sharpless NE. Detecting and characterizing circular RNAs. Nat Biotechnol. 2014;32:453–61.
8. Memczak S, Jens M, Elefsinioti A, Torti F, Krueger J, Rybak A, et al. Circular RNAs are a large class of animal RNAs with regulatory potency. Nature. 2013;495:333–8.
9. Hansen TB, Jensen TI, Clausen BH, Bramsen JB, Finsen B, Damgaard CK, et al. Natural RNA circles function as efficient microRNA sponges. Nature. 2013;495:384–8.
10. Yang Y, Gao X, Zhang M, Yan S, Sun C, Xiao F, et al. Novel role of FBXW7 circular RNA in repressing glioma tumorigenesis. J Natl Cancer Inst. 2018;110:304–15.
11. Li Z, Huang C, Bao C, Chen L, Lin M, Wang X, et al. Exon-intron circular RNAs regulate transcription in the nucleus. Nat Struct Mol Biol. 2015;22:256–64.
12. Naeli P, Pourhanifeh MH, Karimzadeh MR, Shabaninejad Z, Movahedpour A, Tarrahimofrad H, et al. Circular RNAs and gastrointestinal cancers: Epigenetic regulators with a prognostic and therapeutic role. Crit Rev Oncol Hematol. 2020;145:102854.
13. Meng S, Zhou H, Feng Z, Xu Z, Tang Y, Li P, et al. CircRNA: functions and properties of a novel potential biomarker for cancer. Mol Cancer. 2017;16:94.
14. Zhang J, Hou L, Liang R, Chen X, Zhang R, Chen W, et al. CircDLST pomotes the tumorigenesis and metastasis of gastric cancer by sponing miR-502-5p and activating the NRAS/MEK1/ERK1/2 signaling. Mol Cancer. 2019;18(1):80.
15. Liu H, Liu Y, Bian Z, Zhang J, Zhang R, Chen X, et al. Circular RNA YAP1 inhibits the proliferation and invasion of gastric cancer cells by regulating the miR-367-5p/p27kip1 axis. Mol Cancer.

2018;17(1):151.
16. Wang KW, Dong M. Role of circular RNAs in gastric cancer: recent advances and prospects. World J Gastrointest Oncol. 2019;11(6):459–569.
17. Kristensen LS, Hansen TB, Veno MT, Kjems J. Circular RNAs in cancer: opportunities and challenges in the field. Oncogene. 2018;37(5):555–65.
18. Naeli P, Poirthanifeh MH, Karimzadeh MR, Shabaninejad Z, Movahedpour A, Tarrahimofrad H, et al. Circular RNAs and gastrointestinal cancers: Epigenetic regulators with a prognostic and therapeutic role. Crit Rev Oncol Hematol. 2020;145:102854.
19. Abbaszadeh-Goudarzi K, Radbakhsh S, Pourhanifeh MH, Khanbabaei H, Davoodvandi A, Fathizadeh H, et al. Circular RNA and diabetes: epigenetic regulator with diagnostic. Curr Mol Med. 2020 Jan 29. doi:10.2174/1566524020666200129142106.
20. Han B, Chao J, Yao H. Circular RNA and its mechanisms in disease: from the bench to the clinic. Pharmacol Ther. 2018;187:31–44.
21. Chen S, Li T, Zhao Q, Xiao B, Guo J. Using circular RNA hsa_circ_0000190 as a new biomarker in the diagnosis of gastric cancer. Clin Chim Acta. 2017;466:167–71.
22. Tian M, Chen R, Li T, Xiao B. Reduced expression of circRNA hsa_circ_0003159 in gastric cancer and its clinical significance. J. Clin. Lab. Anal. 2018; 32(3).
23. Lu J, Zhang PY, Xie JW, Wang JB, Lin JX, Chen QY, et al. Hsa_circ_0000467 promotes cancer progression and serves as a diagnostic and prognosis biomarker for gastric cancer. J Clin Lab Anal. 2019;33(3):e22726.
24. Li P, Chen S, Chen H, Mo X, Li T, Shao Y, et al. Using circular RNA as a novel type of biomarker in the screening of gastric cancer. Clin Chim Acta. 2015;444:132–6.
25. Tang W, Fu K, Sun H, Rong D, Wang H, Cao H. CircRNA microaaray profiling identifies a novel circulating biomarker for detection of gastric cancer. Mol Cancer. 2018;17(1):137.
26. Zhong S, Wang J, Hou J, Zhang Q, Xu H, Hu J, et al. Circular RNA Hsa_circ_0000993 inhibits metastasis of gastric cancer cells. Epigenomics. 2018;10(10):1301–13.
27. Hu B, Ying X, Wang J, Piriyapongsa J, Jordan IK, Sheng J, et al. Identification of a tumor-suppressive human-specific microRNA within the FHIT tumor-suppressor gene. Cancer Res. 2014;74(8):2283–94.
28. Li J, Zhen L, Zhang Y, Zhao L, Liu H, Cai D, et al. Circ_104916 is downregualted in gastric cancer and suppresses migration and invasion of gastric cancer cells. Onco Ther. 2017;10:3521–29.
29. Zhang J, Liu H, Hou LD, Wang G, Zhang R, Huang YX, et al. Circular RNA_LARP4 inhibits cell proliferation and invasion of gastric cancer by sponging miR-424-5p and regulationg LATS1 expression. Mol Cancer. 2017;16:151.
30. Cheng J, Zhuo H, Xu M, Wang L, Xu H, Peng J, et al. Regulatory network of circRNA-miRNA-mRNA contributes to the histological classification and disease progression in gastric cancer. J Transl Med. 2018;16(1):216.

31. Zheng Q, Bao C, Guo W, Li S, Chen J, Chen B, et al. Circular RNA profiling reveals an abundant circHIPK3 that regulates cell growth by sponging multiple miRNAs. Nat Commun. 2016;7:11215.
32. Wang K, Long B, Liu F, Wang JX, Liu CY, Zhao B, et al. A circular RNA protects the heart from pathological hypertrophy and heart failure by targeting miR-223. Eur Heart J. 2016;37:2602–11.
33. Yu DL, Zhang C. Circular. RNA PTK2 Accelerates Cell Proliferation and Inhibits Cell Apoptosis in Gastric Carcinoma via miR-139-3p. Dig Dis Sci. 2020. Doi:10.1007/s10620-020-06358-4.
34. Zhang L, Huang P, Li Q, Wang D, Xu CX. miR-134-5p promotes stage I lung adenocarcinoma metastasis and chemoresistance by targeting DAB2. Mol Ther Nulriv Acids. 2019;18:627–37.
35. Fu D, Lu C, Qu X, Li P, Chen K, Shan L, et al. LncRNA TTN-AS1 regulates osteosarcoma cell apoptosis and drug resistance via the miR-134-5p/MBTD1 axis. Aging. 2019;11(19):8374–85.
36. Glisovic T, Bachorik JL, Yong J, Dreyfuss G. RNA-binding proteins and post-transcriptional gene regulation. FEBS Lett. 2008;582(14):1977–86.
37. Ladd AN, Charlet N, Cooper TA. The CELF family of RNA binding proteins is implicated in cell-specific and developmentally regulated alternative splicing. Mol Cell Biol. 2001;21(4):1285–96.
38. Subramaniam D, Natarajan G, Ramalingam S, Ramachandran I, May R, Queimado L, et al. Translation inhibition during cell cycle arrest and apoptosis: Mcl-1 is a novel target for RNA binding protein CUGBP2. Am J Physiol Gastrointest Liver Physiol. 2008;294(4):G1025-32.
39. Mukhopadhyay D, Houchen CW, Kennedy S, Dieckgraefe BK, Anant S. Coupled mRNA stabilization and translational silencing of cyclooxygenase-2 by a novel RNA binding protein, CUGBP2. Mol Cell. 2003;11(1):113–26.
40. de la Rosa J, Weber J, Friedrich MJ, Li Y, Rad L, Ponstingl H, et al. A single-copy Sleeping Beauty transposon mutagenesis screen identifies new PTEN-cooperating tumor suppressor genes. Nat Genet. 2017;49(5):730–41.
41. Yeung YT, Fan S, Lu B, Yin S, Yang S, Nie W, et al. CELF2 suppresses non-small cell lung carcinoma growth by inhibiting the PREX2-PTEN interaction. Carcinogenesis. 2019;Pii:bgz113.
42. Long ZW, Wu JH, Cai-Hong, Wang YN, Zhou Y. MiR-374b promotes proliferation and inhibits apoptosis of human GIST cells by inhibiting PTEN through activation of the PI3K/Akt pathway. Mol cells. 2018;41(6):532–44.

Figures

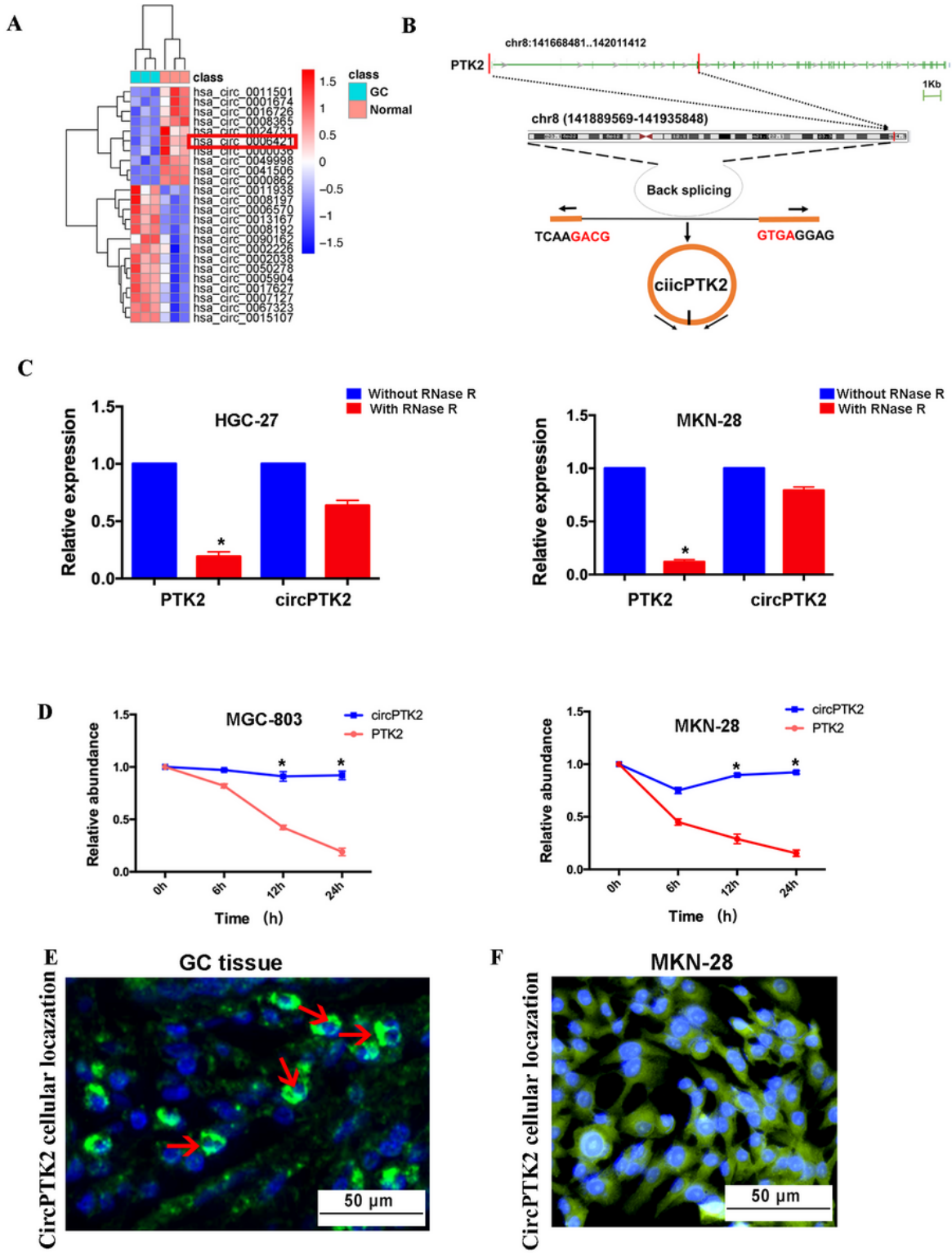

Figure 1

Identification and characteristics of circPTK2 in GC cells. A. A circRNA microarray was used to identify the differentially expressed circRNAs between GC and normal tissues. B. Genomic loci of PTK2 and circPTK2; circPTK2 is named has_circ_0006421 (chr8:141889569-141935848). C. Quantitative real-time PCR (qRT-PCR) analysis of the enrichment levels of circPTK2 and PTK2 after treatment with RNase R in HGC-27 and MKN-28 cells. D. qRT-PCR analysis of the half-life of circPTK2 and PTK2 after treatment with

actinomycin D at the indicated time points in MGC-803 and MKN-28 cells. E. RNA fluorescence in situ hybridization (FISH) analysis of the cellular localization of circPTK2 in GC tissues and MKN-28 cells. Blue color: DAPI; green color: circPTK2; arrows: circPTK2. *P < 0.05. Abbreviations: GC gastric cancer.

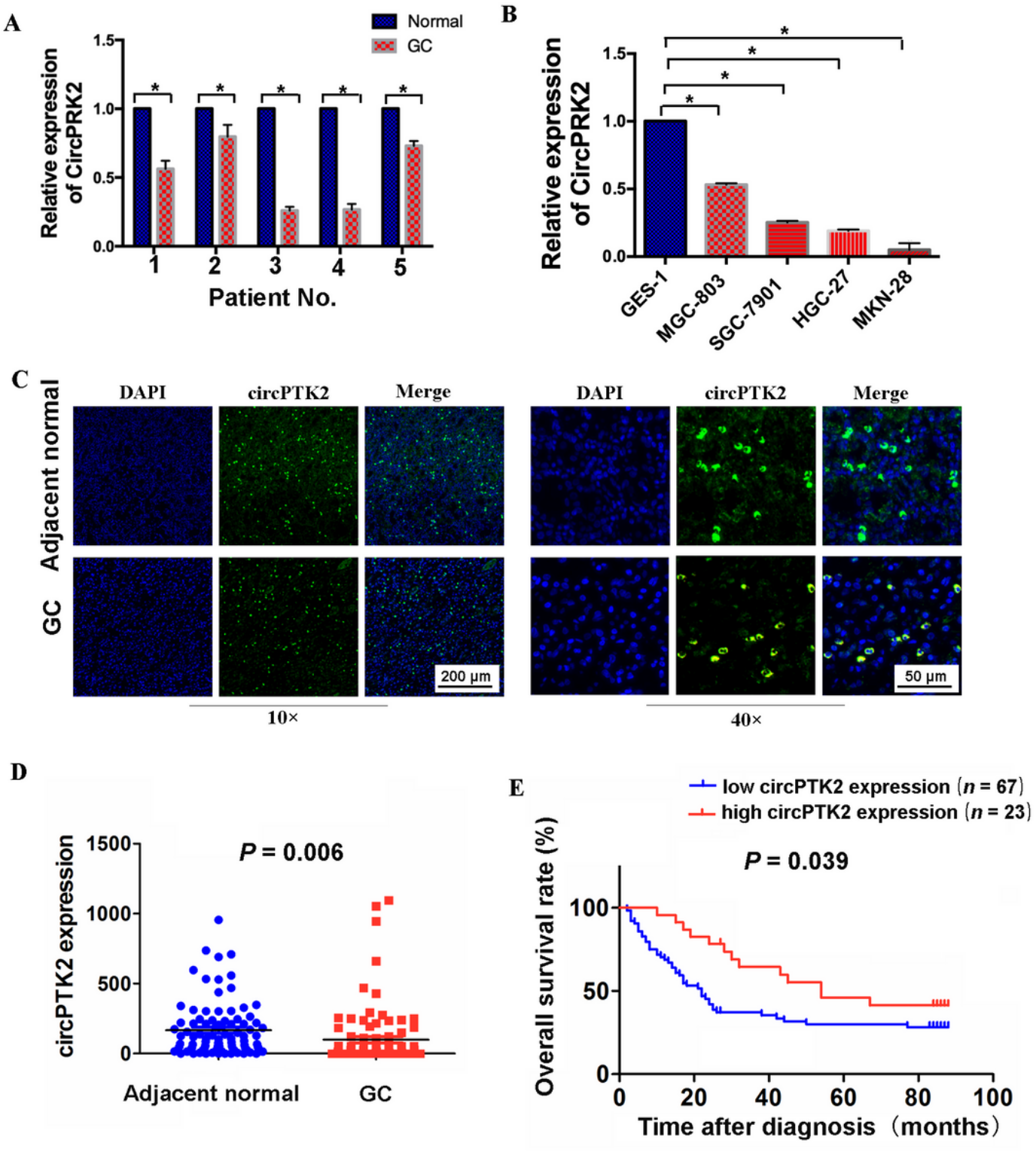

Figure 2

Association between circPTK2 expression and OS of GC patients. A. Expression levels of circPTK2 are significantly lower in GC tissues than in paired adjacent normal tissues. B. Expression levels of circPTK2

are lower in GC cell lines (MKN28, MGC803, SGC-7901, and HGC-27) than in the normal gastric mucosa cell line GES-1. C, D. FISH analysis of the expression of circPTK2 in 90 GC tissue samples. E. Kaplan-Meier analysis of the association of circPTK2 expression with OS of GC patients. Abbreviations: OS: overall survival; GC：gastric cancer.

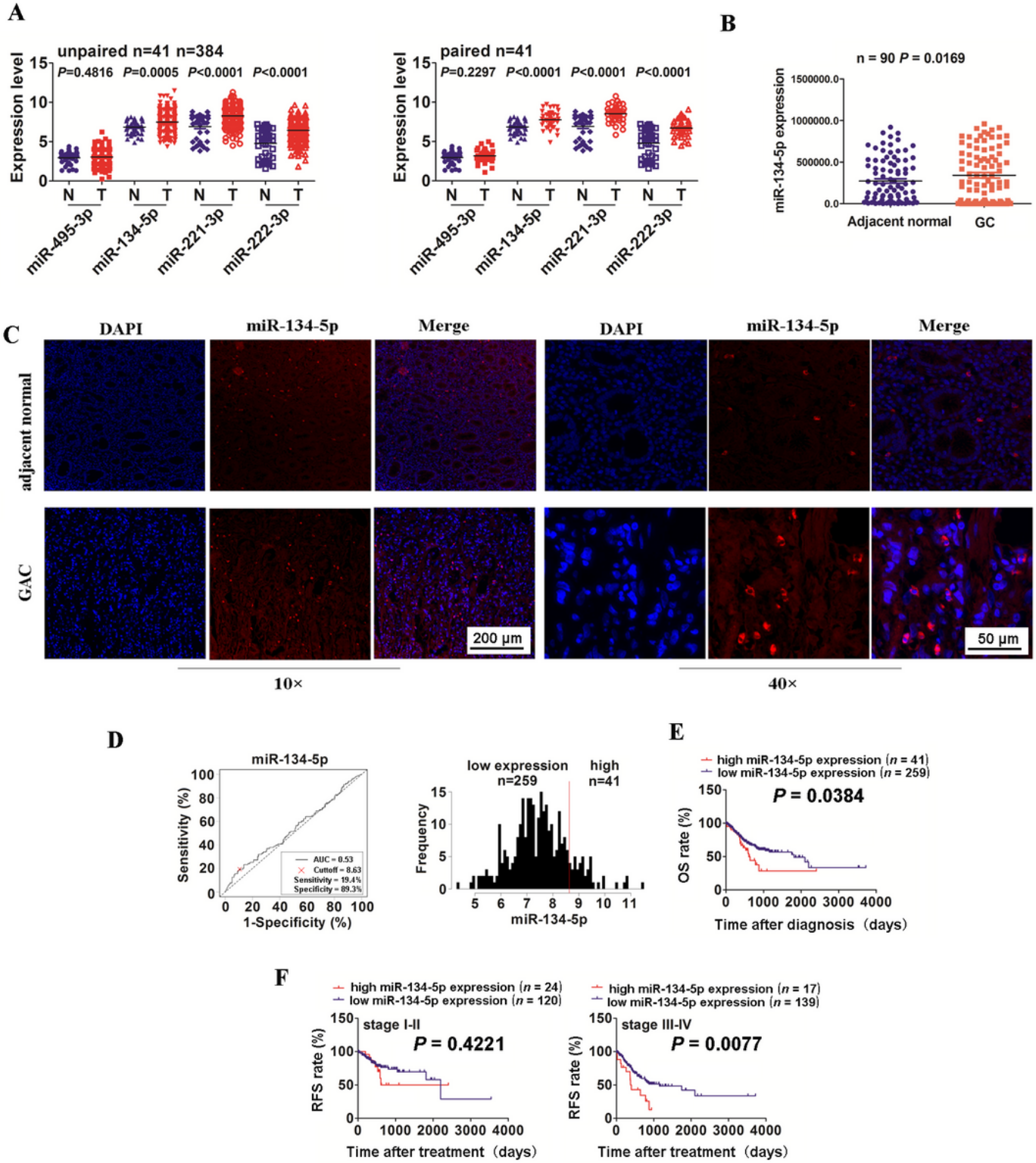

Figure 3

Correlation of miR-134-5p expression with OS and RFS of GC patients. A. TCGA analysis of the expression levels of four miRNAs in 384 cases including 41 paired GC tissues. B, C. FISH analysis of the expression levels of miR-134-5p in 90 paired GC tissue samples. D. ROC curve analysis of the cutoff value of miR-134-5p expression used to divide patients into high and low miR-134-5p expression groups. E. Kaplan-Meier analysis of the correlation of miR-134-5p expression with OS of GC patients. F. Kaplan-Meier analysis of the correlation of miR-134-5p expression with RFS of GC patients. Abbreviations: OS: overall survival; RFS: recurrence-free survival; GC gastric cancer; TCGA: The Cancer Genome Atlas; FISH: Fluorescence in situ hyburdization; ROC: Receiver operating characteristic.

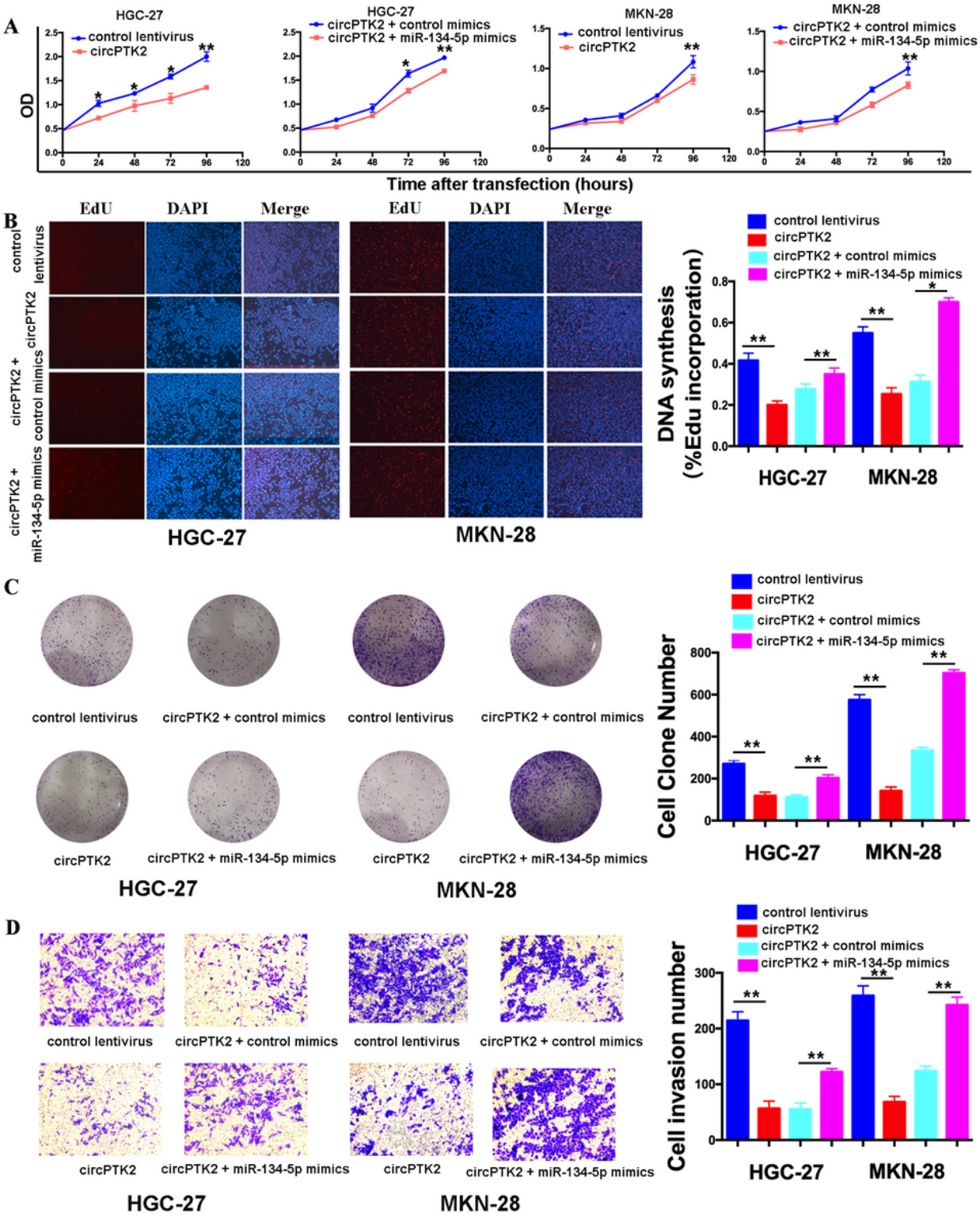

Figure 4

circPTK2 inhibits the proliferation, DNA synthesis, colony formation, and invasion of GC cells. A. CCK8 analysis of the cell viability after transfection with circPTK2 overexpression plasmids and/or miR-134-5p mimics in HGC-27 and MKN-28 cell lines. B. EdU analysis of the DNA synthesis after transfection with circPTK2 overexpression lentivirus and/or miR-134-5p mimics in HGC-27 and MKN-28 cell lines. C. Assessment of cell colony formation abilities after transfection with circPTK2-overexpression plasmids

and/or miR-134-5p mimics in HGC-27 and MKN-28 cell lines. D. Transwell assay of the cell invasive capabilities after transfection with circPTK2-overexpression plasmids and/or miR-134-5p mimics in HGC-27 and MKN-28 cell lines. Data represent the means ± SEM of three experiments. *P < 0.05, **P < 0.01. Abbreviations: GC：gastric cancer.

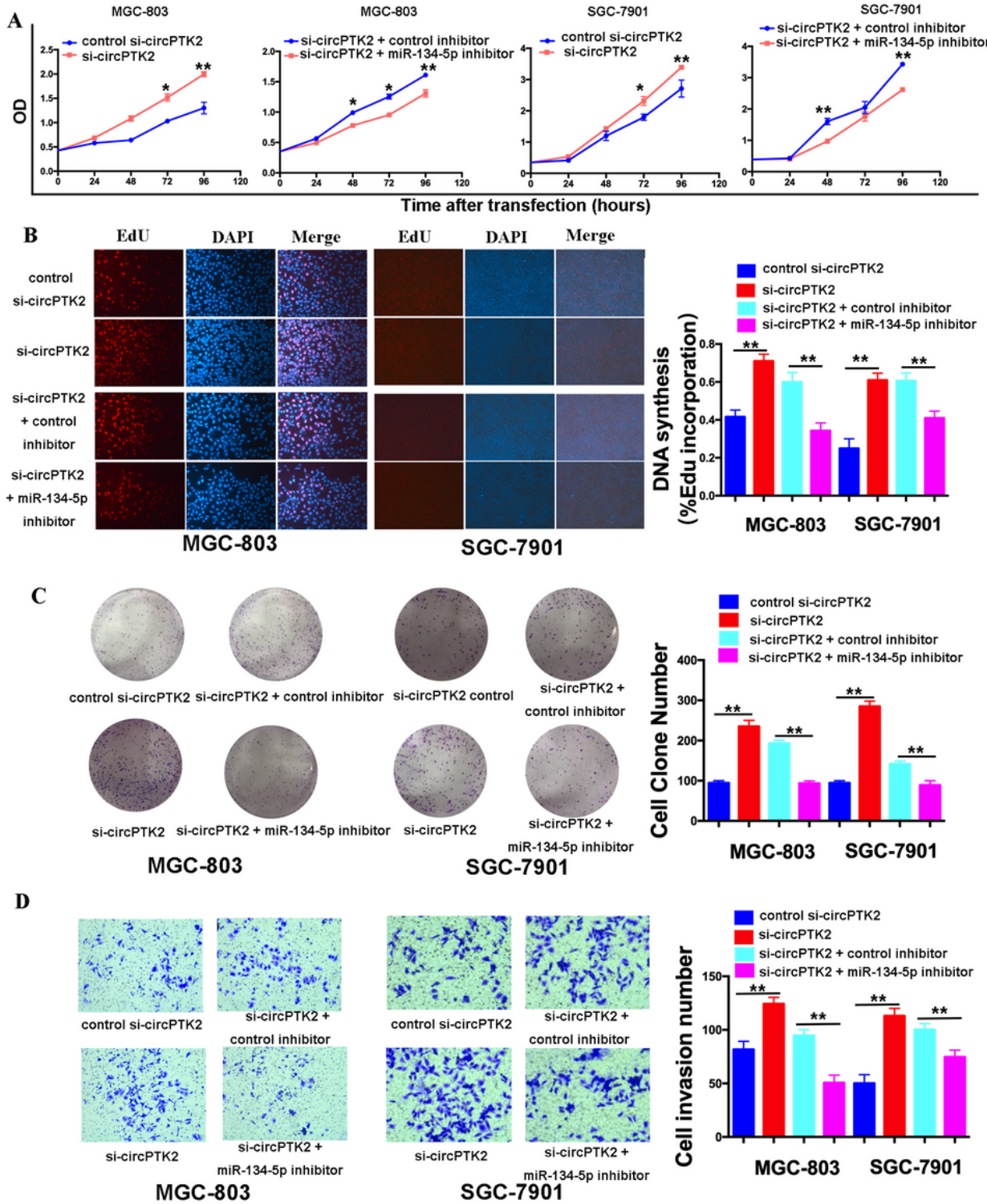

Figure 5

Knockdown of circPTK2 promotes the proliferation, DNA synthesis, colony formation, and invasion of GC cells. A. CCK8 analysis of the cell viability after transfection with sh-circPTK2 and/or miR-134-5p inhibitor in MGC-803 and SGC-7901 cell lines. B. EdU analysis of the DNA synthesis after transfection with sh-circPTK2 and/or miR-134-5p inhibitor in MGC-803 and SGC-7901 cell lines. C. Assessment of cell colony formation ability after transfection with si-circPTK2 and/or miR-134-5p inhibitor in MGC-803 and SGC-7901 cell lines. D. Transwell assay of cell invasive capabilities after transfection with si-circPTK2 and/or miR-134-5p inhibitor in MGC-803 and SGC-7901 cell lines. Data represent the mean ± SEM of three experiments. *P < 0.05, **P < 0.01. Abbreviations: GC gastric cancer.

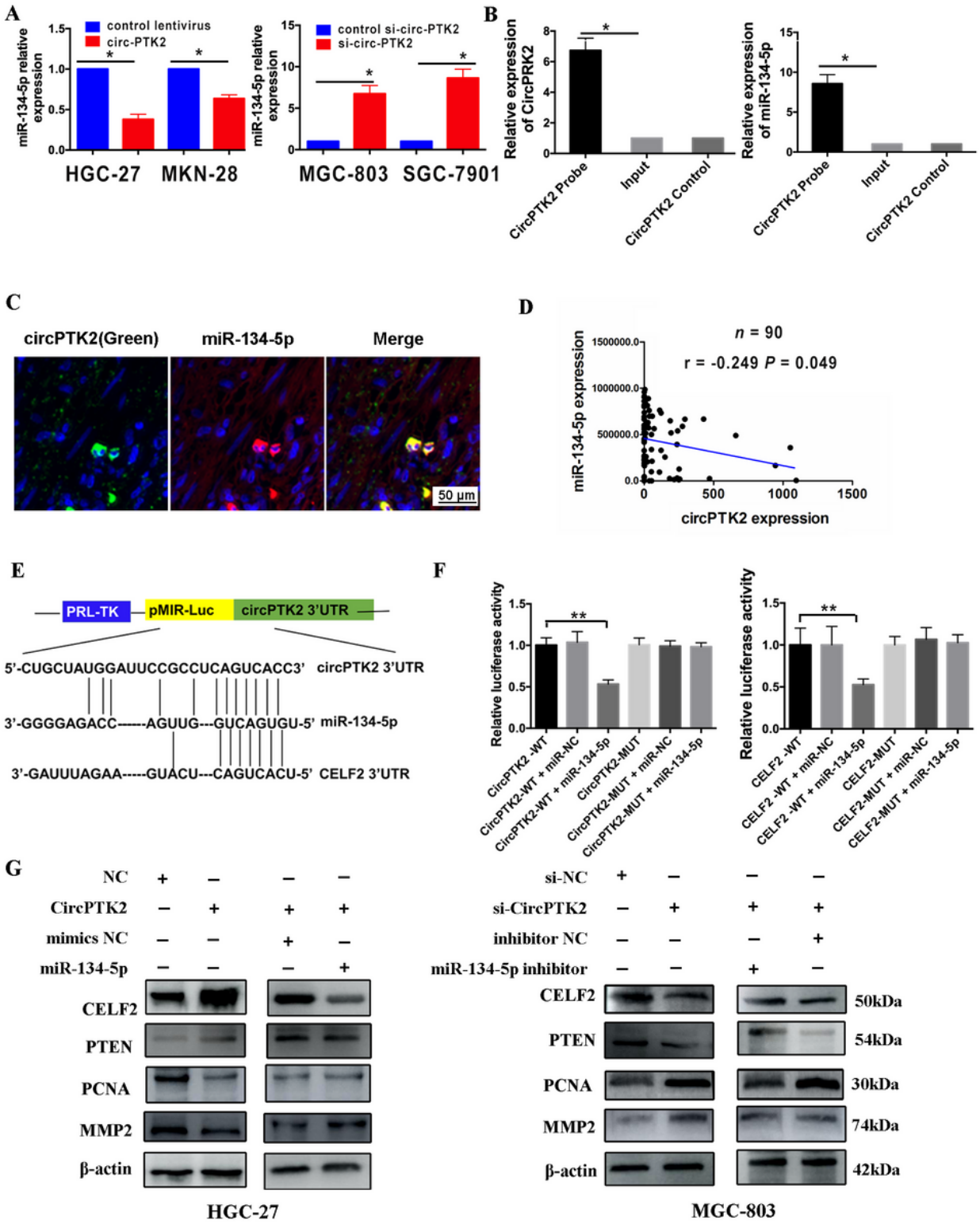

Figure 6

circPTK2 acts as a sponge of miR-134-5p to activate the CELF2/PTEN signaling in GC cells. A. Expression levels of miR-134-5p in circPTK2-overexpressing HGC-27 and MKN-28 cells and si-circPTK2-transfected MGC-803 and SGC-7901 cells. B. circRNA in vivo precipitation analysis of the purified RNA pulled down by a circPTK2-specific probe and qRT-PCR analysis of the enrichment levels of circPTK2 and miR-134-5p in HGC-27 cells. C. circPTK2 is co-localized with miR-134-5p in the cytoplasm of GC cells.

Green: circPTK2; red: miR-134-5p; yellow: merge. D. Pearson correlation analysis of the correlation of miR-134-5p with circPTK2 expression in 90 GC tissues. E. Schematic representation of the potential binding sites between circPTK2 and miR-134-5p and between miR-134-5p and CELF2. F. The luciferase activity of wild-type (WT) luc-circPTK2/luc-CELF2 and mutant (Mut) luc-circPTK2/luc-CELF2 after co-transfection with miR-134-5p mimics in HEK297T cells. G. Western blotting analysis of the activity of CLEF2/PTEN signaling after the co-transfection of circPTK2-overexpression vectors and/or miR-134-5p mimics in HGC-27 cells and after the co-transfection of si-circPTK2 and/or miR-134-5p inhibitor in MGC-803 cells. Data represent mean ± SEM from three experiments. *P < 0.05, **P < 0.01. Abbreviations: GC gastric cancer qRT-PCR quantitative real-time PCR.

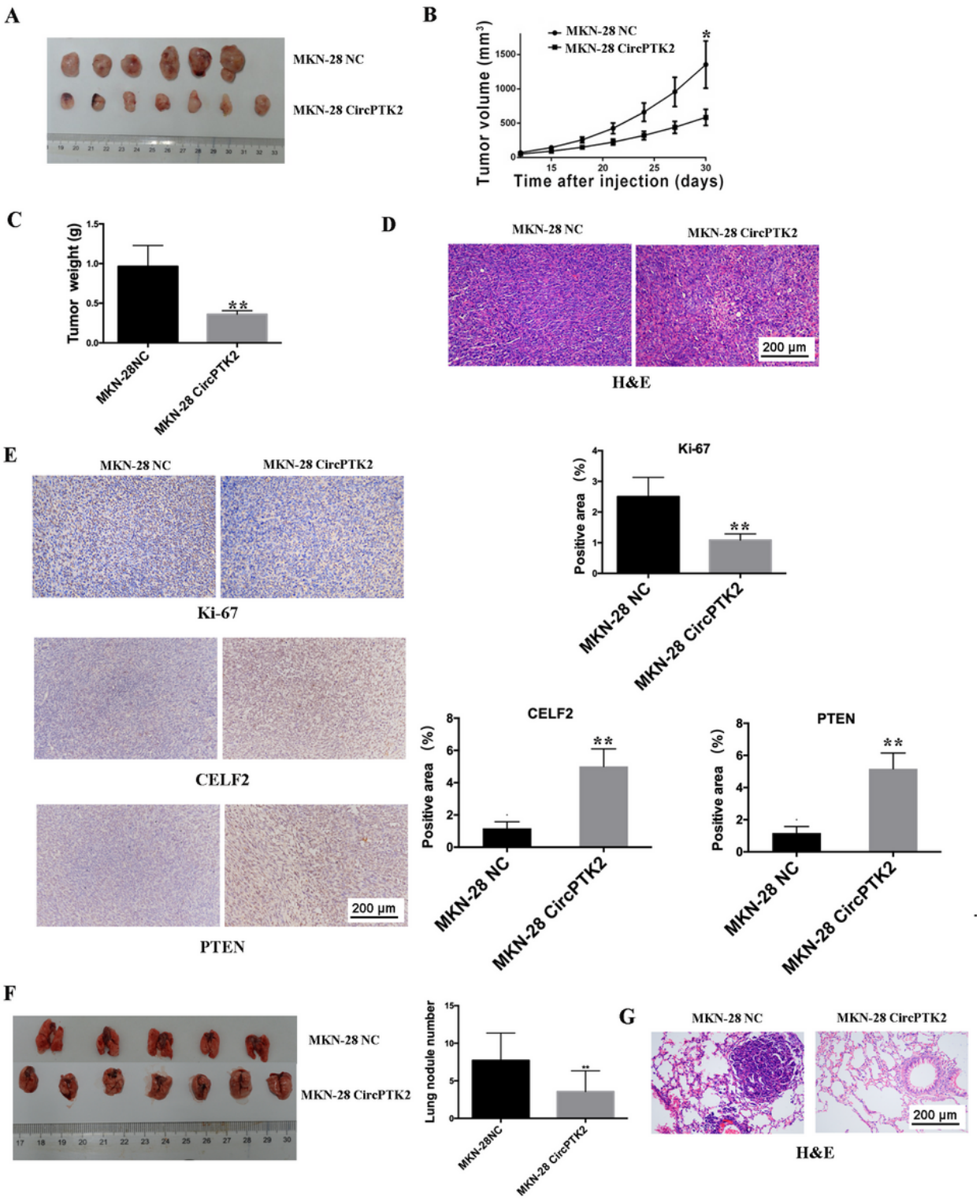

Figure 7

Effects of circPTK2 on in vivo tumor growth and lung metastasis. A. Comparison of the volume of xenograft tumors induced in circPTK2 overexpression and NC groups. B. Tumor growth in circPTK2 overexpression and NC groups. C. Comparison of the tumor weights in circPTK2 overexpression and NC groups. D. HE analysis of tumor cell numbers in circPTK2 overexpression and NC groups. E. Immunohistochemical analysis of Ki-67, CELF2, and PTEN indexes in xenograft tumor tissues between

circPTK2 overexpression and NC groups. F. Comparison of the lung metastatic tumors in circPTK2 overexpression and NC groups. G. HE analysis of the metastatic tumor cell numbers in circPTK2 overexpression and NC groups. Data are expressed as mean ± SEM. *P < 0.05, **P < 0.01. Abbreviations: NC: negative control; HE: Hematoxylin-eosin.

Figure 8

Schematic representation of the proposed mechanism of circPTK2 in GC cells. circPTK2 acted as a sponge of miR-134-5p to active CELF2/PTEN and down-regulate PCNA and MMP2 expression, leading to the suppression of GC tumorigenesis and metastasis. Abbreviations: GC gastric cancer.

Supplementary Files

This is a list of supplementary files associated with this preprint. Click to download.

- Fig.S1.tif
- Fig.S2.tif
- Fig.S3.tif
- Fig.S4.tif
- SupplementaryFigureLegendsandtables.docx